J. Am. Soc. Mass Spectrom. (2011) 22:1052–1062
DOI: 10.1007/s13361-011-0102-3

RESEARCH ARTICLE

# Negative Ion CID Fragmentation of *O*-linked Oligosaccharide Aldoses—Charge Induced and Charge Remote Fragmentation

Roisin A. Doohan,[1] Catherine A. Hayes,[2] Brendan Harhen,[1] Niclas Göran Karlsson[2]

[1]School of Chemistry, National University of Ireland, Galway, Ireland
[2]Department of Medical Biochemistry, University of Gothenburg, P.O. Box 440405 30, Gothenburg, Sweden

**Abstract**

Collision induced dissociation (CID) fragmentation was compared between reducing and reduced sulfated, sialylated, and neutral *O*-linked oligosaccharides. It was found that fragmentation of the $[M - H]^-$ ions of aldoses with acidic residues gave unique Z-fragmentation of the reducing end GalNAc containing the acidic C-6 branch, where the entire C-3 branch was lost. This fragmentation pathway, which is not seen in the alditols, showed that the process involved charge remote fragmentation catalyzed by a reducing end acidic anomeric proton. With structures containing sialic acid on both the C-3 and C-6 branch, the $[M - H]^-$ ions were dominated by the loss of sialic acid. This fragmentation pathway was also pronounced in the $[M - 2H]^{2-}$ ions revealing both the C-6 Z-fragment plus its complementary C-3 C-fragment in addition to glycosidic and cross ring fragmentation. This generation of the Z/C-fragment pairs from GalNAc showed that the charges were not participating in their generation. Fragmentation of neutral aldoses showed pronounced Z-fragmentation believed to be generated by proton migration from the C-6 branch to the negatively charged GalNAc residue followed by charge remote fragmentation similar to the acidic oligosaccharides. In addition, A-type fragments generated by charge induced fragmentation of neutral oligosaccharides were observed when the charge migrated from C-1 of the GalNAc to the GlcNAc residue followed by rearrangement to accommodate the $^{0,2}$A-fragmentation. LC-MS also showed that *O*-linked aldoses existed as interchangeable α/β pyranose anomers, in addition to a third isomer (25% of the total free aldose) believed to be the furanose form.

**Key words:** Glycomics, Mass spectrometry, Electrospray, *O*-linked oligosaccharides

## Introduction

*O*-linked glycosylation is one of the key post-translational modifications of secreted and cell surface/bound proteins. It is involved in biological processes such as cancer, infection, and inflammation [1–5]. The most well known *O*-linked glycosylation is the mucin type glycosylation characterized by the linking of GalNAc to Ser/Thr that could be extended into complex structures by C-3 and C-6 elongation of this GalNAc. Usually the structures are based on *N*-acetyllactosamine extensions, terminating in fucose, sialic acid, and sulfate, and quite often ABO blood group antigens can be found on mucin type oligosaccharides [6–8]. *O*-linked oligosaccharides on mucus proteins, the mucins, are the main carriers of blood group ABO antigens in the body and are found on all mucosal surfaces. The mucins provide protection from the hostile environment of the gastrointestinal tract, where highly glycosylated protein regions

**Electronic supplementary material** The online version of this article (doi:10.1007/s13361-011-0102-3) contains supplementary material, which is available to authorized users.

*Correspondence to:* Niclas Karlsson; *e-mail:* niclas.karlsson@medkem.gu.se

Received: 13 October 2010
Revised: 5 February 2011
Accepted: 8 February 2011
Published online: 31 March 2011

of the mucins prevent degrading enzymes from digesting underlying epithelia. Glycosylation of mucins is also responsible for control and entrapment of pathologic bacteria and virus oligosaccharides in the gastrointestinal tract [9–11].

With glycosylation being very sensitive to environmental changes, it is one of the biological parameters that is likely to alter due to diseases [12, 13]. As such, it is predicted that glycobiomarkers can serve as early diagnostics for diseases. The altered glycosylation is also thought to have an impact on how glycoproteins interact with other molecules and influence the outcome of biological threats, for instance in the lung and gastrointestinal surfaces. Many pathogens have been shown to interact with oligosaccharide motifs on *O*-linked oligosaccharides. Hence, this interaction will have to be further studied in order to understand the specificity of various pathogens. Structural characterisations of *O*-linked oligosaccharides are usually carried out after these structures have been released from the proteins. With the lack of enzymatic approaches for the release procedures, researchers must use chemical methods. The most common chemical method is reductive β-elimination, and this approach has been very successful in generating the vast majority of structural information available on *O*-linked glycosylation [14, 15]. However, this aforementioned release approach does not allow efficient studies for the interaction of separated individual oligosaccharide components. This is because the release method turns mucin type oligosaccharide into unstable aldoses before they are reduced and captured as stable alditols. The chemical modification of reduction prevents covalent attachment to solid supports to explore mucin oligosaccharides binding capabilities to various biological binding partners. Hence, various approaches for non-reductive β-elimination have been proposed using both gentle alkaline conditions [16, 17], hydrazinolysis [18, 19], chemical capturing of the reducing end to prevent degradation of released oligosaccharides[20–24], and flow systems that are quickly transporting oligosaccharides to nondegrading environments after they have been released [25, 26]. The generation of *O*-linked oligosaccharide aldoses would allow these structures to be included in glycoarrays and thus used for high throughput screening of oligosaccharide interaction partners [27–30] to generate glycobiomarkers. The reducing end would also allow *O*-linked oligosaccharides to be labeled with fluorophores and chromophores for sensitive detection by HPLC as well as improving their behavior in both mass spectrometry and chromatography [31].

Mass spectrometry has evolved into one of the main approaches for structural characterisation [14, 32–36]. Negative ion mode of native oligosaccharides has been shown to provide sensitive detection as well as very informative fragmentation for structural characterisation. It provides an alternative to advanced glycomic platforms that rely on chemical derivatization on the reducing terminus or permethylation [36], and is conceptionally easier to adopt and implement in many biological mass spectrometric laboratories. Fragmentation rules have been compiled for various types of both acidic and neutral oligosaccharides, including *N*-linked oligosaccharides [37, 38], free milk oligosaccharides [32, 33], and *O*-linked oligosaccharide alditols [39]. The fragmentation spectra of free milk oligosaccharides and *N*-linked aldoses has been shown to give predominantly C-type fragments and cross ring cleavages, while mucin alditols gives predominantly Z-type fragments. However, due to difficulties in generating mucin type *O*-linked aldoses, only a few examples of the fragmentation of these structures in negative ion mode have been presented. Hyphenation of graphitized carbon chromatography with negative ion mode ESI mass spectrometry is currently one of the techniques being investigated in a global evaluation of glycomic platforms [40, 41]. Understanding the negative ion mode fragmentation of *O*-linked aldoses is important, in order to be able to utilize current glycomic platforms for these type of molecules. This report describes how isolated *O*-linked oligosaccharide aldoses, released by an in-flow system, fragment in unique pathways, compared with what has been described for other types of reducing oligosaccharides.

## Methods

### *Generation of Oligosaccharide Alditols and Aldoses*

Oligosaccharide aldoses and alditols were generated from porcine gastric mucins and bovine fetuin (Sigma-Aldrich, St. Louis, MO, USA) (more detailed description in Supplementary material). Aldoses were released from 10 mg of protein according to the in-line flow method [25] by capturing oligosaccharides in neutral conditions on a graphitized carbon cartridge. Further purifications of NeuAcα2-3Galβ1-3GalNAc, Galβ1-3(NeuAcα2-6)GalNAc, NeuAcα2-3Galβ1-3(NeuAcα2-6)GalNAc, and NeuAcα2-3Galβ1-3(NeuAcα2-3Galβ1-4GlcNAcβ1-6)GalNAc from bovine fetuin were carried out using anion exchange. The reducing fetuin oligosaccharide mixtures obtained from the in-line release method were injected in milliQ $H_2O$ onto a 7.5×75 mm Prosphere P-WAX 10 u, 1000 Å column (Alltech, Deerfield, IL, USA) connected to an Alliance 2695 HPLC (Waters, Milford, MA, USA) coupled to a ELS detector (Sedere, Alfortville, France) system using 100% MilliQ $H_2O$ for 11 min followed by a gradient increase to 30% 0.5 M ammonium acetate, pH 5.0 over the next 25 min. One min fractions were collected and pooled according to the HPLC trace and MS oligosaccharide confirmation. Alditols from the same glycoproteins were released by reductive β-elimination. Galβ1-3(Galβ1-4GlcNAcβ1-6)GalNAc was generated from NeuAcα2-3Galβ1-3(NeuAcα2-3Galβ1-4GlcNAcβ1-6)GalNAc after desialylation [10]. Fucα1-2Galβ1-3($HSO_3$-6GlcNAcβ1-6)GalNAc and Fucα1-2Galβ1-3(Fucα1-2Galβ1-4($HSO_3$-6)GlcNAcβ1-6)GalNAc from porcine gastric mucin were subjected to mass spectrometry without further purification, since these structures are isomeri-

cally pure in this sample [9]. See Supplementary Materials section for further experimental detail.

### *Desialylation of the Core 2 1329 Oligosaccharide Ion*

One nmol of the oligosaccharide in 14 µL of milliQ $H_2O$ was added to a solution of 4 µL of 250 mM sodium phosphate, pH 6.0 buffer, and 2 µL of Sialidase A and incubated at 37°C overnight. The resulting solution was purified over a 150 mg Carbograph SPE cartridge as indicated in the supplementary information using 10 mM $NH_4HCO_3$ and 80% ACN, 10 mM $NH_4HCO_3$ in place of 0.1% TFA, and 80% acetonitrile (ACN), 0.1% trifluoroacetic acid (TFA). The oligosaccharide was then lyophilized.

### *ESI-MS of Oligosaccharides*

Samples were analyzed in negative ion mode on an Agilent LC/MS XCT Ultra Ion Trap (Agilent, Santa Clara, CA, USA) either with direct infusion (10 µg/mL with a flow rate of 5 µL/min in 10 mM ammonium bicarbonate in 40% acetonitrile) or by graphitzed carbon LC-MS using HPLC 1100 Series system with an autosampler [10]. The samples were chromatographed using a PGC column (300 µm× 100 mm) (Thermo Electron West Palm Beach , FL, USA) and a linear gradient up to 40% of 10 mM ammonium hydrogen carbonate/80% acetonitrile, followed by a two minute gradient to 80% acetonitrile. The ionization parameters for the ESI probe were set as follows: capillary voltage of −151 V, skimmer of −40 V, Oct1 DC of −12 V and Oct2 DC of −2.7 V. The drying temperature was maintained at 350 °C, while the dry gas of nitrogen was run at 5.0 L/min with the nebulizer pressure at 10 psi. Collision induced dissociation was performed at 35% normalized collision energy. Accumulated CID spectra have been submitted to the public UniCarb-DB database(www.unicarb-db.com).

## Results

### *CID Charge Remote Fragmentation of Reducing Sulfated O-linked Oligosaccharides*

Porcine gastric mucin is a rich source of well characterized sulfated *O*-linked oligosaccharides, with 6-sulfation on GlcNAc on core two structures [9]. By isolation of the acidic oligosaccharides by anion exchange chromatography, we could observe two dominant masses of *m/z* 811/1119 (aldoses) and *m/z* 813/1121 (alditols) in the ESI-MS corresponding to the sulfated oligosaccharides. LC-MS and LC-$MS^2$ of these reducing and nonreducing oligosaccharides concluded that they were isomerically pure and corresponded to the structures Fucα1-2Galβ1-3($HSO_3$-6GlcNAcβ1-6)GalNAc/ol and Fucα1-2Galβ1-3(Fucα1-2Galβ1-4($HSO_3$-6)GlcNAcβ1-6)GalNAc/ol, respectively.

The $MS^2$ spectra of the sulfated alditols (Figure 1) showed the typical pattern, where more intense peaks for glycosidic fragmentation remote from the sulfated residues are usually seen [42]. The loss of blood group H type fucose to form Y fragments (Domon and Costello fragmentation nomenclature [43] is the dominating ion in both of the spectra of the alditols. Overall, fragmentation of the alditols is also dominated by primary Y type fragmentation (Figure 1c), and accounted for 100% (*m/z* 813) and 81% (*m/z* 1121), respectively, of the total ion counts of the two $MS^2$-spectra. The domination of Y type fragmentation is consistent with what has been described previously in negative mode low energy collision of both Q-TOF and ion trap instruments for sulfated *O*-linked oligosaccharide alditols [44]. The $MS^2$ spectra of both the aldoses on the other hand displayed a dominant Z type fragment from the loss of the C-3 branch of GalNAc, corresponding to the $Z_{1\alpha}$ ions *m/z* 485 (Figure 1a) and *m/z* 793 (Figure 1b) of the smaller and the larger structure, respectively. The fragmentation also includes more cross ring type fragments of 6% (*m/z* 811) and 18% (*m/z* 1119), as well as internal fragments of 18% (*m/z* 811) and 27% (*m/z* 1119) (Figure 1c). No cross ring fragments were observed of the alditols, and internal fragments only consisted of 19 % of multiple Y type fragments for the *m/z* 1121 ion. No multiple Y fragments were observed for the smaller *m/z* 813 structure. The high intensity Z type fragments of the aldoses indicate that while the charge in both the alditol and the aldose is located on the sulfate group and fragmentation of the compounds is via a charge remote pathway, the acidic proton present on the hemiacetal in the case of the aldoses is inducing and/or promoting a particular fragmentation pathway of the reducing end GalNAc, compared with when no acidic protons are present, as is the case of the [M – H] ions of the alditols. The pathway not induced by these anomeric protons appears to progress via Y type fragmentation, and these fragment ions are present in the $MS^2$ spectra of both the alditols and the aldoses, though in the later case with a lower intensity due to the acidic anomeric proton promoting the Z type fragmentation.

### *CID Charge Remote Fragmentation of Reducing Monosialylated O-linked Oligosaccharides*

Fetuin is a rich source of simple sialylated structures, and following oligosaccharide release we found two isomers separated by anion exchange and graphitized carbon chromatography corresponding to the composition $NeuAc_1Hex_1HexNAc_1$. By CID fragementation, it was found that the major component (Figure 2a) had the seqeunce corresponding to the structure NeuAcα2-3Galβ1-3GalNAc previously identified from bovine fetuin [25]. The minor component (Figure 2b) was identified as the desialylated component Galβ1-3(NeuAcα2-6)GalNAc generated during preparation of fetuin from the disialylated component NeuAcα2-3Galβ1-3(NeuAcα2-6)GalNAc found in aboundance in fetuin [25].

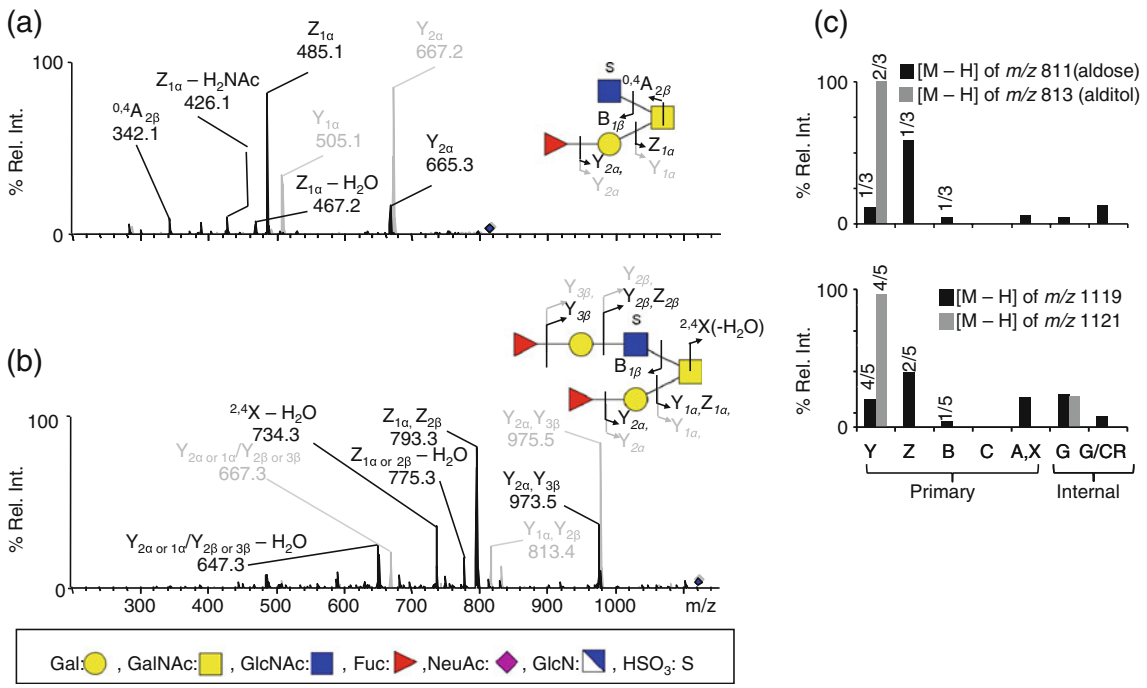


**Figure 1.** Comparisons of the $MS^2$ fragmentation of reducing and non-reducing sulfated *O*-linked oligosaccharides. Overlaid $MS^2$ spectra of both the reducing, shown in black, and non-reducing ions, shown in grey, of both Fucα1-2Galβ1-3($HSO_3$-6GlcNAcβ1-6)GalNAc ($[M - H]^-$ ions of *m/z* 811 and 813) (**a**), and Fucα1-2Galβ1-3(Fucα1-2Galβ1-4($HSO_3$-6)GlcNAcβ1-6) GalNAc ($[M - H]^-$ ions of *m/z* 1119 and 1121) (**b**). Bar charts (**c**) of the relative intensities of the primary and internal fragment ions observed for (**a**) (upper) and (**b**) (lower). Y, Z, B, C, A, and X represent primary fragments and G and G/CR represent the internal fragments from both glycosidic (G) and glycosidic/cross ring (CR) fragments. The ratios above the bar graph represent the number of experimental glycosidic fragments (Y, Z, B, or C) detected in relation to the theoretical number of glycosidic fragments from each group. Below the figures is the key for monosaccharide residue representation

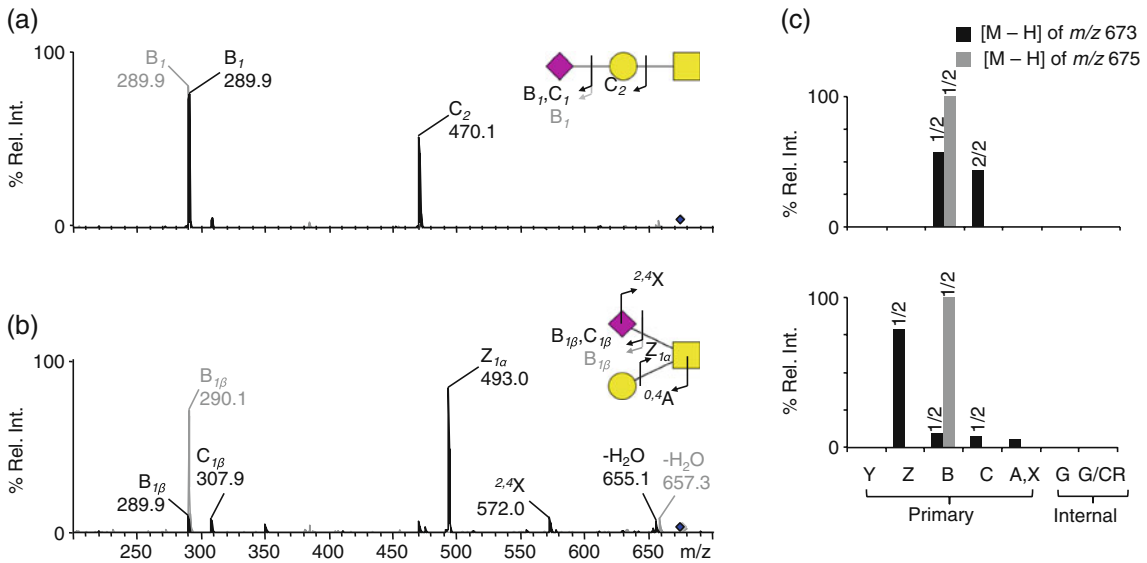


**Figure 2.** Comparisons of the $MS^2$ fragmentation of reducing and non-reducing monosialylated isomeric *O*-linked oligosaccharides. Overlaid $MS^2$ spectra of both the reducing, shown in black, and non-reducing ions, shown in grey, of NeuAcα2-3Galβ1-3GalNAc (**a**), and Galβ1-3(NeuAcα2-6)GalNAc (**b**). Precursor ions of $[M - H]^-$ ions of *m/z* 673 and 675), respectively. Bar charts (**c**) of the relative intensities of the primary and internal fragment ions observed for (**a**) (upper) and (**b**) (lower). See Figure 1 for bar chart, monosaccharide key explanations

Both sialic acid and sulfate will be the main carriers of the negative charge in negative ion ESI-MS, but due to the lability of sialic acid compared with sulfate in negative ion mode fragmentation [36], it was anticipated that the fragmentation of sialylated *O*-linked oligosaccharide aldoses would be transmitted via different and/or additional pathways to the sulfated structures. The lability of sialic acid in fragmentation was obvious as the major $MS^2$ fragment of the NeuAcα2-3Galβ1-3GalNAc aldose was shown to be the $B_1$ fragment ion of *m/z* 290 from NeuAc, and this was also the major fragment of the corresponding alditol (Figure 2a). In addition, the NeuAcα2-3Galβ1-3GalNAc aldose also displayed a major $C_2$ fragment of *m/z* 470, and these two fragments dominated the spectrum (Figure 2a). With the charge localized to sialic acid on the C-3 branch of the GalNAc, as opposed to the sulfate on the C-6 branch as described previously, the $C_2$ fragment corresponds to the same fragmentation pathway of the reducing end GalNAc, previously described as the major fragmentation pathway for the sulfated structures giving the abundant Z type ions. Because of the charge remote mechanism, the fragmentation of the bonds will render one charged fragment and one neutral fragment and, depending on the location of the charge on the C-3 or C-6 of the GalNAc moiety, the major fragment ion will correspondingly be from either of the branches, where the C-6 branch fragment will also contain the GalNAc. The suggestion that the fragmentation of the reducing end into C and Z fragments of the GalNAc is the major generic pathway for charge remote fragmentation of acidic *O*-linked oligosaccharide aldoses in negative mode is further supported by the fragmentation of the Galβ1-3(NeuAcα2-6)GalNAc structure. With the sialic acid instead located to the C-6, the $Z_{1\alpha}$ fragmentation catalyzed by the acidic proton on the reducing end GalNAc is again the most pronounced fragment, so much so that it is by far more aboundant then the $B_{1\beta}$ fragment of *m/z* 290 from the labile sialic acid (Figure 2b). The absence of a reducing end transmitted fragmentation made the sequencing of the two corresponding trisaccharide alditols difficult. Only low abundant glycosidic fragment ions was detected except the $B_1$ from sialic acid (Figure 2a and b). This suggests that negative ion ESI-MS CID fragmentation of aldoses provides more informative $MS^2$ spectra compared with the alditols in regards to acidic *O*-linked oligosaccharides.

## *CID Charge Remote Fragmentation of Reducing Disialylated O-linked Oligosaccharides*

Fetuin also contains the disialylated species NeuAcα2-3Galβ1-3(NeuAcα2-6)GalNAc and NeuAcα2-3Galβ1-3(NeuAcα2-3Galβ1-4GlcNAcβ1-6)GalNAc [25]. Now, with two acidic groups in the molecule these ions can be deteced both as singly charged $[M - H]^-$-ions (*m/z* 964/966 and 1329/1331 of aldose/alditol) and doubly charged $[M - 2H]^{2-}$-ions (*m/z* 482/483 and 664/665, aldose/alditol). In the case of of the $MS^2$ spectra of the singly charged species (Figure 3a and c), it is obvious that the introduction of an acidic proton associated with sialic acid has further destabilized the sialic acid glycosidic bonds by providing a mobile proton to the proximity of these bonds. The presence of the acidic anomeric protons in the singly charged spectra provides an alternative pathway to the GalNAc Z/C fragmentation described above. This alternative fragmentation is the loss of the remaining uncharged sialic acid giving the Y fragment ions of *m/z* 673 from the tetrasaccharide and *m/z* 1038 from the hexasaccharide, respectively. The $Z_{1\alpha}$ ions of *m/z* 493 and 858 in the spectra of the small and large aldose and the $C_2$ ion *m/z* 470 of low intensity, (4% and 3%, respectively) is also seen in both spectra (Figure 3b and d), identifying the composition of the C-6 and C-3 branches of the GalNAc. The CID-spectra of the singly charged [M – H] ions of the alditols only showed consecutive loss of sialic acids ($Y_{2\alpha}$, $Y_{3\beta}$ of *m/z* 1040 and $Y_{2\alpha}/Y_{3\beta}$ of *m/z* 749) before further fragmentation of the backbone could be detected. This made the localization of sialic acid impossible from CID of the alditols alone.

For the doubly charged $[M - 2H]^{2-}$-ions of the aldoses, one charge is located at each of the antennas of the C-3 and C-6 branch of the disialylated structures. The only acidic proton left is then located at the GalNAc moitey, and fragmentation from the reducing end via the charge remote GalNAc Z/C fragmentation (described earlier) is predicted to be dominating (Figure 3b and d). The disialyled tetrasaccharide is producing the major fragments of $C_{2\alpha}$ with *m/z* 470 and $Z_{1\alpha}$ with *m/z* 493 from the doubly charged $[M - 2H]^{2-}$-ion of *m/z* 482 splitting the parent ion into two fragments (Figure 3b). The same fragmentation pathway is also seen for the disialylated hexasaccharides, where the $C_2$ with *m/z* 470 and $Z_1$ with *m/z* 858 from the doubly charged $[M - 2H]^{2-}$-ion of *m/z* 664 displayed increased intensity compared with the fragmentation of its singly charged equivalent, (Figure 3d). However, the pathway of $Y_1$ type fragmentation (loss of sialic acid) is dominating the spectra (*m/z* 1038). Hence, it looks like the stability of the sialic acid glycosidic bond decreases as the molecular weight increases as detected by the slight increase of the $B_1$ ion *m/z* 290 and the $Y_1$ ions of *m/z* 1038 of the doubly charged hexasaccharide aldose (Figure 3d) compared with the $B_1$ ion *m/z* 290 and the $Y_1$ ion of *m/z* 673 (Figure 3b) of the tetrasaccharide aldose. These Y fragments (*m/z* 675/1040) and the $B_1$ fragments from sialic acid (*m/z* 290) for the tetra-/hexasaccharide were also the dominating fragments of the doubly charged alditols (Figure 3b and d), but without dominating Z/C fragmentation of the reducing end GalNAc as seen in the aldoses.

## *CID Fragmentation of Neutral Reducing O-linked Oligosaccharides*

With the highly acidic charges such as sulfate and sialic acid removed from the molecule, the most likely localization of the charge on neutral oligosaccharide aldoses would occur as a result of the removal of the acidic anomeric proton in

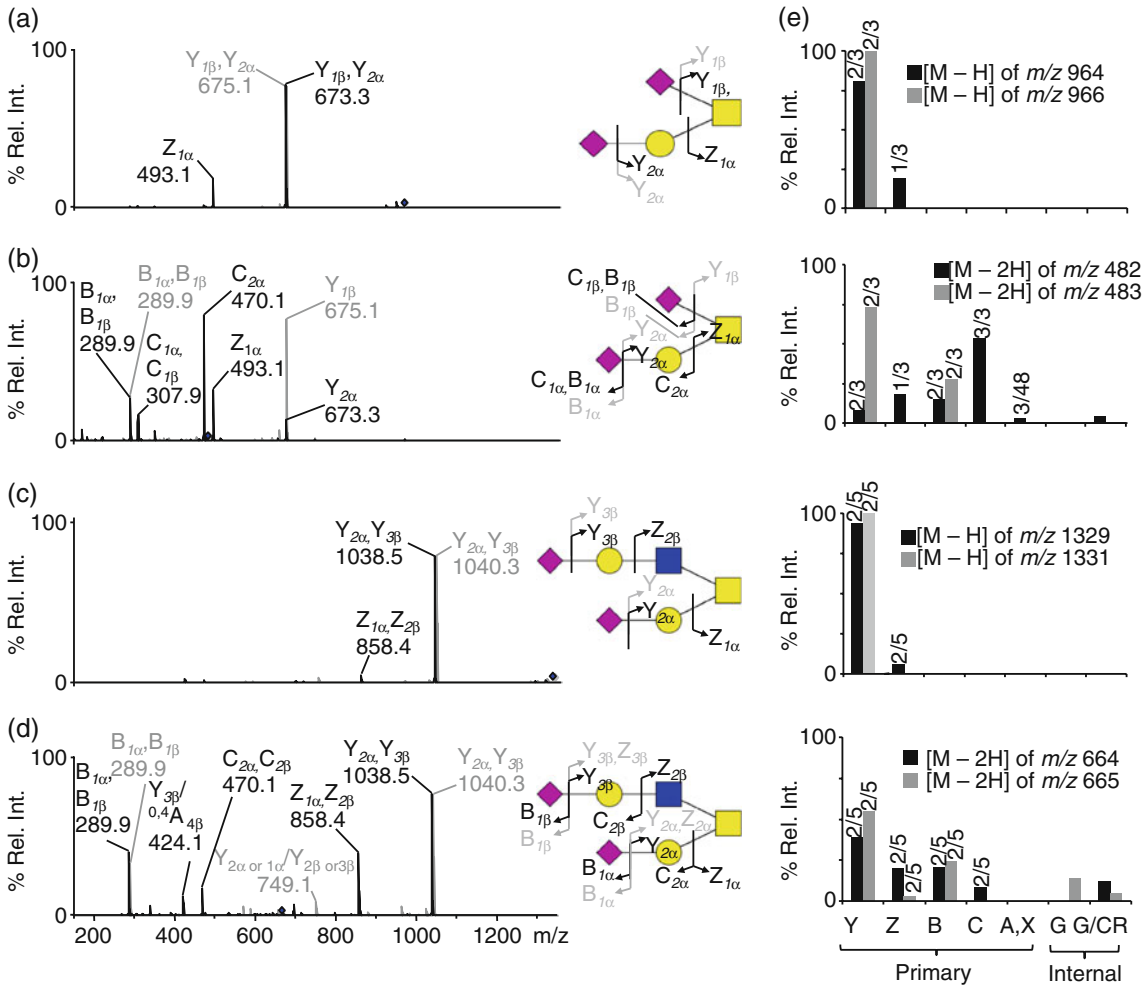


**Figure 3.** Comparisons of the $MS^2$ fragmentation of reducing and non-reducing disialylated *O*-linked oligosaccharides. Overlaid $MS^2$ spectra of both the reducing, shown in black, and non-reducing ions, shown in grey, of both the singly charged ($[M - H]^-$ ions of *m/z* 964 and 966) and doubly charged ($[M - 2H]^{2-}$ ion of *m/z* 482 and 483) NeuAcα2-3Galβ1-3(NeuAcα2-6) GalNAc, (**a**) and (**b**), and the singly charged ($[M - H]^-$ ions of *m/z* 1329 and 1331) and doubly charged ($[M - 2H]^{2-}$ ion of *m/z* 664 and 665) NeuAcα2-3Galβ1-3(NeuAcα2-3Galβ1-4GlcNAcβ1-6)GalNAc, (**c**) and (**d**). Bar charts (**e**) of the relative intensities of the primary and internal fragment ions observed. See Figure 1 for bar chart and monosaccharide key explanations

negative ion ESI-MS. This process has been indicated to make the $[M - H]^-$ ions unstable and undergo in-source fragmentation [25]. This was also observed in this study, where the mass spectrometric settings optimized for acidic oligosaccharides needed to be modified for the neutral oligosaccharide aldoses (but not for alditols) by increased desolvation gas flow and capillary temperature (data not shown).

Previous fragmentation studies of neutral milk oligosaccharides in negative ion mode ESI-MS have shown that the fragmentation progresses occurs via a charge induced fragmentation originating from the reducing end, producing C type fragments [33], but preliminary studies of *O*-linked oligosaccharide aldoses under similar conditions have indicated that fragmentation progresses via a different pathway [25]. After optimization of the ion source settings, we detected the two parent ions of the structures Galβ1-3(Galβ1-4GlcNAcβ1-6) GalNAc (desialylated from fetuin, $[M - H]^-$-ion of *m/z* 747) and Fucα1-2Galβ1-3(Fucα1-2Galβ1-4GlcNAcβ1-6)GalNAc (porcine gastric mucin, $[M - H]^-$-ion of *m/z* 1039). It was found that the CID fragmentation (Figure 4) produced fragment masses identical to the those observed by in-source fragmentation of the aldoses, as previously seen [25]. The information poor spectra, which detected only two fragment ions in each of the cases, were in stark contrast with the $MS^2$ spectra produced by the equivalent alditols and from reported fragmentation of milk oligosaccharides, with Glc at the reducing end instead of GalNAc. Assignment of the fragments showed that one of them was again the $Z_1$ fragment of the GalNAc moiety [*m/z* 567 in Figure 4a and *m/z* 713 in Figure 4b], previously detected as the major fragement generated by charge remote fragmentation of the charge localised to the C-6 branch. The only other fragment was that of *m/z* 424 assigned as the $^{0,4}A$ fragment, showing again that the reducing end GalNAc is very sensitive to fragmentation.

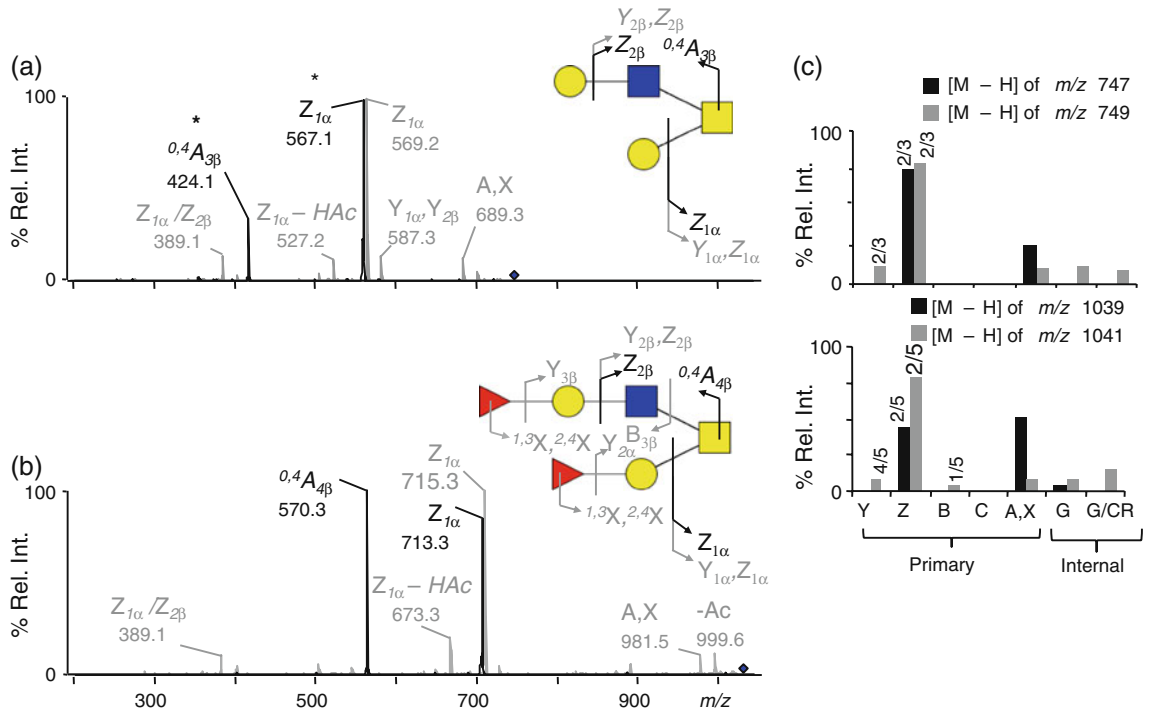


**Figure 4.** Comparisons of the $MS^2$ fragmentation of reducing and non-reducing neutral *O*-linked oligosaccharides. Overlaid $MS^2$ spectra of both the reducing, shown in black, and non-reducing ions, shown in grey, of both Galβ1-3(Galβ1-4GlcNAcβ1-6) GalNAc ($[M - H]^-$ ions of *m/z* 747 and 749) (**a**) and Fucα1-2Galβ1-3(Fucα1-2Galβ1-4GlcNAcβ1-6)GalNAc ($[M - H]^-$ ions of *m/z* 1039 and 1041) (**b**). Bar charts of the relative intensities of the primary and internal fragment ions observed (**c**). See Figure 1 for bar chart and monosaccharide key explanations

## *Charge Remote and Charge Induced Fragmentation of Reducing O-Linked Oligosaccharides*

In order to further characterize the fragments generated by CID of the neutral oligosaccharides, the $^{0,4}A$ fragment of *m/z* 424 and the $Z_{1\alpha}$ fragment of *m/z* 567 from the CID of the $[M - H]^-$-ion from Galβ1-3(Galβ1-4GlcNAcβ1-6)GalNAc were subjected to $MS^3$ fragmentation (Figure 5a and b, respectively). The dominating $MS^3$ fragment of the $Z_{1\alpha}$ ion was shown to be the $^{0,4}A$ ion of *m/z* 424, indicating that this is a fragment ion formed by the concomitant fragmentation of the initially formed $Z_{1\alpha}$ ion shown throughout this report to be a dominating fragment of reducing end GalNAc and formed by charge remote fragmention, where the charge is located on the C-6 branch of the GalNAc. That this is indeed a charge remote fragmentation is further substantiated by performing CID of a reducing monosaccharide already precharged on the C-6 location. The [M – H] ion of GlcN-6$SO_3$H fragmented into two major ions of *m/z* 199 ($^{1,3}X$) and *m/z* 139 ($^{0,4}A$), where the presence of the latter showed that $^{0,4}A$ fragmentation was formed by charge remote fragmentation when the C-6 branch is charged (Figure 5c). It was also shown that substituting the C-6 with methyl groups on monosaccharides did not give $^{0,4}A$ fragmentation (data not shown), showing that the charge localization to the C-6 branch is a prerequisite for $^{0,4}A$ fragmentation.

For the neutral *O*-linked oligosaccharide aldoses this means that the mechanism for forming the $^{0,4}A$ fragment has also to involve a charge migration, since the most acidic protons initially removed in the ESI giving the [M – H] ions are the ones located to C-1 on the reducing end GalNAc.

With a mechansim of charge migration-charge remote fragmentation shown to be one of the main mechanisms for the formation of $^{0,4}A$ fragments of neutral mucin oligosaccharides, it could also be asked if there is evidence for charge induced fragmentation of reducing neutral mucin oligosaccharides, similar to what has been proposed for other reducing neutral oligosaccharides [33]. A closer look into the $MS^3$ fragment spectrum of the $Z_{1\alpha}$ fragment ion of *m/z* 567.1 showed low amounts of fragment ions. Figure 5b shows an expansion by 40-fold in the low mass region in order to see the low intensity ions in addition to the high abundant $^{0,4}A$ fragment of *m/z* 424. In particular, there were two cross ring fragments detected ($^{0,2}A_2$ of *m/z* 281 and $^{0,2}A_2 - H_2O$ of *m/z* 263). This type of fragmentation has previously been shown to be indicative of C-4 substituted neutral oligosaccharides, both reducing and reduced [14, 32, 33]. Since these fragments were not found when the C-6 branch was precharged with acidic residues such as sialic acid (Figures 2 and 3), it could be suggested that these diagnostic cross ring fragments are generated by charged induced fragmentation pathways. In the $MS^3$ fragment spectrum of the $Z_{1\alpha}$ precursor ion of *m/z* 567, it is evident that charge

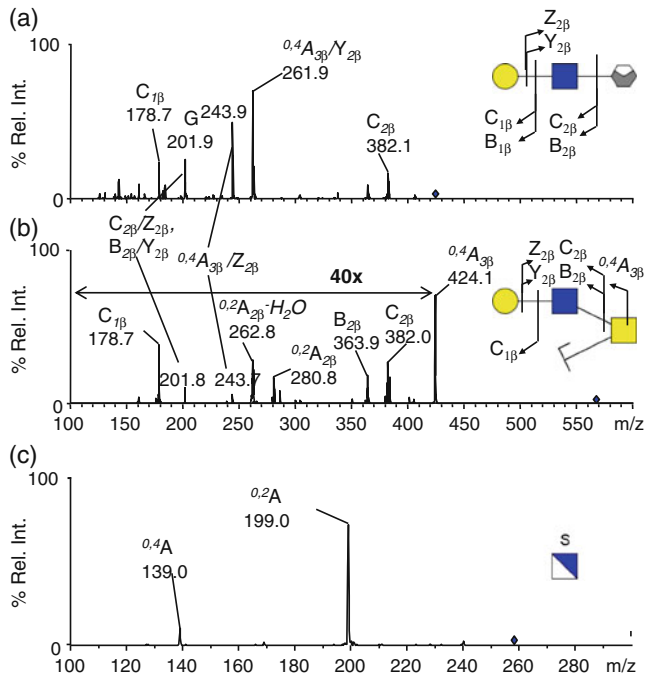


**Figure 5.** Evidence to explain charge remote and charge induced fragmentation. $MS^3$ fragmentation of the $^{0,4}$A fragment ion of *m/z* 424 (**a**) [*labeled in Figure 4(a)] and the Z fragment ion of *m/z* 567 (**b**) [*labeled in Figure 4(a)], observed from the $MS^2$ spectrum of the $[M - H]^-$ ion Galβ1-3(Galβ1-4GlcNAcβ1-6)GalNAc oligosaccharide. $MS^2$ spectrum of $HSO_3$-6GlcN($[M - H]^-$ ion ($[M - H]^-$ ion of *m/z* 259) (**c**). See Figure 1 for the monosaccharide key explanations. The hexagon at the reducing end in (a) represents the remnants of the reducing end GalNAc after $^{0,4}$A-cross ring fragmentation where the shaded area represents deleted part of the ring due to fragmentation

migration/charge remote fragmentation is dominating. The negative charge from the initially formed C-1 oxygen of GalNAc is migrating to somewhere on the C-6 branch, followed by the charge remote $^{0,4}$A fragmentation (dominating fragment ion *m/z* 424 in Figure 5b) and (Scheme 1a, Supplementary Material). However, a small portion of the $Z_{1\alpha}$ fragment ions may also constitute ions where no migration has occurred and the charge remains on C-1 or, alternatively, it may have located to one of the other electronegative atoms (N or O) within the GalNAc moiety. In this case, a charge driven fragmentation will promote the generation of a C type fragment ion containing only the C-6 branch, similar to the mechanism previously described [33] (Supplementary Scheme 1b). This C-type ion with a negative charge on the newly generated reducing end can undergo additional rearrangements and charge migration to give the $^{0,2}$A fragments of *m/z* 281 and 263 (Scheme 1b). The migration of charge from C-1 of the GlcNAc to C-3 (Supplementary Scheme 1b) of the *m/z* 382 ion explains why this fragmentation is possible for C-4 substituted GlcNAc and not for C-3. However, it would be predicted to happen also for C-6 substituted compunds (data not shown). The absence of chargeable oxygens on the reducing end remnants of the $^{0,4}$A fragment ion *m/z* 424 (described in Scheme 1) explains why this ion does not generate charge remote induced $^{0,2}$A fragments in $MS^3$ (Figure 5a).

The generation of the Z type charge remote fragment of neutral *O*-linked oligosaccharides is not dependent on a reducing end acidic anomeric proton, since it is present in the spectra of the alditols (Figure 4) [14]. In a similar manner, the aldose form is not necessary for the generation of the $^{0,2}$A fragments since it can also be seen in the *O*-linked alditols [14]. However in that case, the charge induced mechanism is probably the same, possibly by the charge initially located on C-4 as described in Supplementary Scheme 1b.

## *Separation of Reducing O-Linked Oligosaccharides by Graphitized Carbon Liquid Chromatography*

Separation of *O*-linked oligosaccharide alditols has shown to be easily accomplished using graphitized carbon chromatography [9, 10, 14, 34]. For *O*-linked aldoses this is more complicated. Figure 6 shows the chromatograms of three of the sialylated species, 675/966/1331 (alditols) and 673/964/1329 (aldoses). The major difference between the reduced and nonreduced forms of the sugars is the change in retention time with the aldoses eluting later than the alditols. This indicates that the confirmation of the reducing end is important for the interaction with the stationary phase. What is also obvious is that the alditols elute in one single peak, whereas the aldoses have a very different profile showing three peaks, two of which are linked. This can be explained

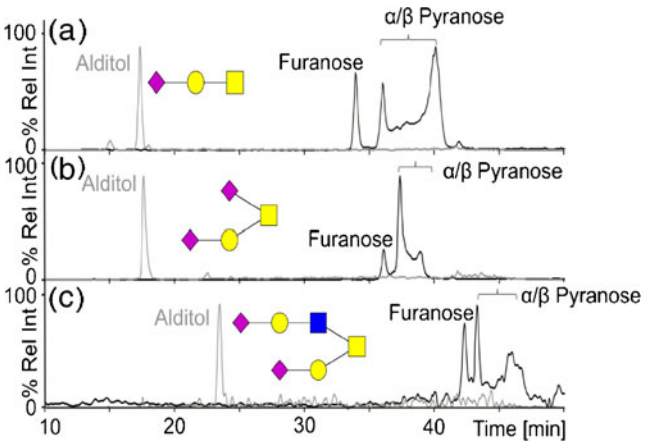


**Figure 6.** Separation of reducing *O*-linked oligosaccharides by graphitized carbon liquid chromatography. The LC-MS chromatograms of reducing furanose and pyranose oligosaccharide forms in black, and non-reducing oligosaccharide alditols in grey. (**a**) Shows the linear monosialylated Galβ1-3(NeuAcα2-6)GalNAc, while (**b**) and (**c**) both show disialylated oligosaccharides, NeuAcα2-3Galβ1-3(NeuAcα2-6)GalNAc and NeuAcα2-3Galβ1-3(NeuAcα2-3Galβ1-4GlcNAcβ1-6)GalNAc, respectively. See Figure 1 for the monosaccharide key explanations

by the fact that when sugars are in the aldose form, there are actually a number of species present in solution [45]. These forms are mutarotations between the open form and the closed ring pyranose and furanose forms of the reducing end sugar. Since the reducing end plays a significant part in the interaction with graphitized carbon, all the different reducing end conformations will be separated fully or partially by the chromatography.

## Discussion

The data in this report indicate that charge remote fragmentation is the main type of fragmentation of *O*-linked oligosaccharide aldoses in negative ion mode. In the case of sulfated and sialylated oligosaccharides, the charge is of course held by these acidic groups, while the fragmentation is happening on other areas of the parent ion. In the case of the neutral oligosaccharides, the fragmentation process is more complex. The charge is initially believed to be generated in the ESI process at the reducing end, since the anomeric proton is the most acidic. During the fragmentation, protons from other areas of the parent ion are migrating to the reducing end, localizing the charge to multiple sites on the molecule. This process is probably dependent on conformation and thus how close other protons can get to the C-1 of the reducing end GalNAc. The data shown for the neutral oligosaccharides in this report indicate that the main branch for charge migration is the C-6 of the GalNAc. This type of elongation of the reducing end is differentiating *O*-linked aldoses from other reducing oligosaccharides previously analyzed in negative ion mode, and this feature is probably responsible for the unique Z-type fragmentation of *O*-linked aldoses shown here. The free rotation of the C5-C6 carbons of the GalNAc, allows the C-6 branch to move into close proximity to the anomeric C-1 position compared to the steric restrictions associated with branches attached to C-3 or C-4. Charge-migration/charge remote fragmentation is probably the dominating mechanism for neutral *O*-linked aldoses while, for instance, in free milk oligosaccharides charge induced fragmentation is dominating [33]. However, charge induced fragmentation plays an important role for determining the linkage configuration of *N*-acetyllactosamine extensions via the generation of the $^{0,2}$A fragments from type 2 chains. Since this type of fragmentation has been shown to be reduced also for acidic milk and N-linked oligosaccharides in negative mode [38], it suggests that the process is charged induced. Scheme 1 (Supplementary Material) proposes the mechanism for how $^{0,2}$A fragments are generated from the Z fragment by the charge induced generation of a C fragment containing the C-6 branch with a charge localised to C-1 of the reducing end monosaccharide of this fragment. With the formation of this ion, subsequent exchange of the proton between C-1 to C-3 promotes the fragmentation into the $^{0,2}$A fragments of *m/z* 281 and *m/z* 263. For acidic oligosaccharides, the charge migration from the acidic group to generate a C-3 charged GlcNAc residue is thermodynamically unfavored and makes the formation of $^{0,2}$A fragments less likely.

The chemistry of reducing *O*-linked oligosaccharides is obviously different compared with other reducing type oligosaccharides. The data in this report (Figure 6) suggest that the already high amount of the furanose form in free Gal [45] compared with other hexoses is increased by C-2*N*-acetylation [46] and substitution on C-3 and C-6. The data in Figure 6 can be interpreted based on results from previous HPLC analysis where the low temperature (0–4 °C) that allowed the separation of pyranose anomers of Gal, still did not separate the fast interconverting furanose anomers of Gal [46]. This was due to the 10 to 35 times faster ring-opening rates of furanoses compared with pyranoses [47]. A reflection of this is seen in the early eluting single peak of unresolved furanoses seen in the chromatograms (Figure 6). The second set of peaks (linked by a shoulder) would therefore be the slow inteconverting α-pyranose and β-pyranose forms. Our data also suggest that there exists a five-carbon and six carbon ring-like intermediate for the furanose and puranose interconversion respectively. The scheme presented by Angyal [46] needs to be further refined with a slow interconversion between these two open chain ring-like intermediates to explain the lack of any shoulder between the furanose and pyranose forms of the reducing sugar in Figure 6. This leads to the observation that several forms of reducing end GalNAc have to be considered if *O*-linked reducing oligosaccharides are used for binding studies, following covalent coupling to solid supports. The oligosaccharides would be coupled via non-natural forms of the reducing end GalNAc, and interaction with other molecules may be altered due to artificially generated molecular structures, not resembling the structures that are present in nature.

## Conclusions

This study has allowed us to present the CID fragmentation of *O*-linked aldoses in negative mode as predominantly charge remote primary fragmentation with the acidic anomeric proton providing alternative fragmentation pathways to the corresponding alditols. A fixed negative charge, as in the case of sulfated and sialylated oligosaccharides, provides superior fragmentation of aldoses compared with alditols for structural elucidation. A prerequisite for informative fragmentation of acidic oligosaccharides is that the number of negative charges of the parent ion corresponded to the number of acidic groups of the oligosaccharide. The fragmentation of the $[M - H]^-$ ions of neutral aldoses and alditols is different. In those cases, a charge migration/remote fragmentation mechanism provides less informative fragments only within the reducing end GalNAc in respect of the aldoses, while informative fragmentation of the alditols allowed the primary sequence to be assigned. The fragmentation of *O*-linked aldoses in negative ion mode is different from other natural oligosaccharide aldoses reported.

This is attributed to the chemical properties of the reducing end GalNAc and its substitution pattern. The chemical anomaly of GalNAc also provides an altered distribution of reducing end conformations. In addition to the anomeric α/β pyranose, the furanose form is also present in a substantial amount. The presence of all these forms may influence the CID fragmentation.

## Acknowledgments

The authors acknowledge support for this research by a combined grant from the Industrial Development Authority, Ireland and Bristol-Myers Squibb. Professor Angela V. Savage is acknowledged for hosting this research effort.

## References

1. Dwek, M.V., Ross, H.A., Leathem, A.J.: Proteome and glycosylation mapping identifies post-translational modifications associated with aggressive breast cancer. *Proteomics* **1**(6), 756–762 (2001)
2. Davis, B. G. Recent Developments in Glycoconjugates. *J. Chem. Soc. Perkin Trans. 1* **22**, 3215–3237 (1999)
3. Kuberan, B., Lindhardt, R.J.: Carbohydrate based vaccines. *Curr. Org. Chem.* **4**(6), 653–677 (2000)
4. Davis, P., Drumm, M., Konstan, M.: Cystic fibrosis. *Am. J. Respir. Crit. Care Med.* **154**(5), 1229–1256 (1996)
5. Varki, A.: Biological roles of oligosaccharides: all of the theories are correct. *Glycobiology* **3**(2), 97–130 (1993)
6. Varki, A., Cummings, R., Esko, J., Freeze, H., Hart, G., Marth, J.: *Essentials of Glycobiology*; Cold Spring Harbor (NY), 1999.
7. Takasaki, S., Yamashita, K., Kobata, A.: The sugar chain structures of ABO blood group active glycoproteins obtained from human erythrocyte membrane. *J. Biol. Chem.* **253**(17), 6086–6091 (1978)
8. Karlsson, N.G., Nordman, H., Karlsson, H., Carlstedt, I., Hansson, G. C.: Glycosylation differences between pig gastric mucin population: a comparative study of the neutral oligosaccharides using mass spectrometry. *Biochem. J.* **326**, 911–917 (1997)
9. Thomsson, K.A., Karlsson, N.G., Hansson, G.C.: Liquid chromatography-electrospray mass spectrometry as a tool for the analysis of sulfated oligosaccharides from mucin glycoproteins. *J. Chromatogr. A* **854**(1/2), 131 (1999)
10. Karlsson, N.G., Wilson, N.L., Wirth, H.J., Dawes, P., Joshi, H., Packer, N.H.: Negative ion graphitised carbon nano-liquid chromatography/mass spectrometry increases sensitivity for glycoprotein oligosaccharide analysis. *Rapid Commun. Mass Spectrom.* **18**, 2282–2292 (2004)
11. Devine, P.: L.; I. F. C. M. Mucins: Structure, function, and associations with malignancy. *BioEssays* **14**(9), 619–625 (1992)
12. Durand, G., Seta, N.: Protein glycosylation and diseases: blood and urinary oligosaccharides as markers for diagnosis and therapeutic monitoring. *Clin. Chem.* **46**(6), 795–805 (2000)
13. Taylor-Papadimitriou, J., Epenetos, A.A.: Exploiting altered glycosylation patterns in cancer: progress and challenges in diagnosis and therapy. *Trends Biotech.* **12**(6), 227–233 (1994)
14. Schulz, B.L., Packer, N.H., Karlsson, N.G.: Small-scale analysis of *O*-linked oligosaccharides from glycoproteins and mucins separated by gel electrophoresis. *Anal. Chem.* **74**(23), 6088–6097 (2002)
15. Spiro, R.G., Bhoyroo, V.D.: Structure of the O-glycosidically linked carbohydrate units of fetuin. *J. Biol. Chem.* **249**(18), 5704–5717 (1974)
16. Rasilo, M.-L., Renkonen, O.: Mild alkaline borohydride treatment liberates *N*-acetylglucosamine-linked oligosaccharide chains of glycoproteins. *FEBS Lett.* **135**(1), 38–42 (1981)
17. Ogata, S.-I., Lloyd, K.O.: Mild alkaline borohydride treatment of glycoproteins—A method for liberating both N- and *O*-linked carbohydrate chains. *Anal. Biochem.* **119**(2), 351–359 (1982)
18. Patel, T., Bruce, J., Merry, A.H., Bigge, J.C., Wormald, M.R., Parekh, R. B.: Use of hydrazine to release in intact and unreduced form both *N*- and *O*-linked oligosaccharides from glycoproteins. *Biochem.* **32**, 679–693 (1993)
19. Cooper, C.A., Packer, N.H., Redmond, J.W.: The elimination of *O*-linked glycans from glycoproteins under non-reducing conditions. *Glycoconj. J.* **11**(2), 163–167 (1994)
20. Basa, L.J., Spellman, M.W.: Analysis of glycoprotein-derived oligosaccharides by high-pH anion-exchange chromatography. *J. Chromatogr. A* **499**, 205 (1990)
21. Makino, Y., Kuraya, N., Omichi, K., Hase, S.: Classification of sugar chains of glycoproteins by analyzing reducing end oligosaccharides obtained by partial acid hydrolysis. *Anal. Biochem.* **238**(1), 54–59 (1996)
22. Anumula, K.R., Dhume, S.T.: High resolution and high sensitivity methods for oligosaccharide mapping and characterization by normal phase high performance liquid chromatography following derivatization with highly flourescent anthranilic acid. *Glycobiology* **8**, 685–694 (1998)
23. Anumula, K.R.: Advances in fluorescence derivatization methods for high-performance liquid chromatographic analysis of glycoprotein carbohydrates. *Anal. Biochem.* **350**(1), 1 (2006)
24. Grun, C.H., van Vliet, S.J., Schiphorst, W.E.C.M., Bank, C.M.C., Meyer, S., van Die, I., van Kooyk, Y.: One-step biotinylation procedure for carbohydrates to study carbohydrate–protein interactions. *Anal. Biochem.* **354**(1), 54–63 (2006)
25. Karlsson, N.G., Packer, N.H.: Analysis of *O*-linked reducing oligosaccharides released by an in-line flow system. *Anal. Biochem.* **305**(2), 173 (2002)
26. Yamada, K., Hyodo, S., Matsuno, Y.-K., Kinoshita, M., Maruyama, S.-Z., Osaka, Y.-S., Casal, E., Lee, Y.C., Kakehi, K.: Rapid and sensitive analysis of mucin-type glycans using an in-line flow glycan-releasing apparatus. *Anal. Biochem.* **371**(1), 52–61 (2007)
27. Culf, A.S., Cuperlovic-Culf, M., Ouellette, R.J.: Carbohydrate microarrays: survey of fabrication techniques. *OMICS* **10**(3), 289–310 (2006)
28. Feizi, T., Fazio, F., Chai, W., Wong, C.-H.: Carbohydrate microarrays —a new set of technologies at the frontiers of glycomics. *Curr. Opin. Struct. Biol.* **13**(5), 637–645 (2003)
29. Shin, I., Park, S., Lee, M.-R.: Carbohydrate microarrays: an advanced technology for functional studies of glycans. *Chem. Eur. J.* **11**(10), 2894–2901 (2005)
30. Liang, P.-H., Wu, C.-Y., Greenberg, W.A., Wong, C.-H.: Glycan arrays: biological and medical applications. *Curr. Opin. Chem. Biol.* **12** (1), 86–92 (2008)
31. Davies, M.J., Hounsell, E.F.: Comparison of separation modes of high-performance liquid chromatography for the analysis of glycoprotein- and proteoglycan-derived oligosaccharides. *J. Chromatogr. A* **720**(1/2), 227–233 (1996)
32. Chai, W., Piskarev, V., Lawson, A.M.: Branching pattern and sequence analysis of underivatized oligosaccharides by combined MS/MS of singly and doubly charged molecular ions in negative-ion electrospray mass spectrometry. *J. Am. Soc. Mass Spectrom.* **13**(6), 670–679 (2002)
33. Pfenninger, A., Karas, M., Finke, B., Stahl, B.: Structural analysis of underivatized neutral human milk oligosaccharides in the negative ion mode by nano-alectrospray MS(*n*) (Part 1: Methodology). *J. Am. Soc. Mass Spectrom.* **13**(11), 1331–1340 (2002)
34. Thomsson, K.A., Karlsson, H., Hansson, G.C.: Sequencing of sulfated oligosaccharides from mucins by liquid chromatography and electrosprayionization tandem mass spectrometry. *Anal. Chem.* **72**(19), 4543–4549 (2000)
35. Kawasaki, N., Ohta, M., Hyuga, M., Hayakawa, T.: Application of liquid chromatography/mass spectrometry and liquid chromatography with tandem mass spectrometry to the analysis of the site-specific carbohydrate heterogeneity in erythropoietin. *Anal. Biochem.* **285**, 82–92 (2000)
36. Joseph, Z.: Mass spectrometry of oligosaccharides. *Mass Spectrom. Rev.* **23**(3), 161–227 (2004)
37. Harvey, D.J.: Fragmentation of negative ions from carbohydrates: part 1. use of nitrate and other anionic adducts for the production of negative ion electrospray spectra from N-linked carbohydrates. *J. Am. Soc. Mass Spectrom* **16**(5), 622–630 (2005)
38. Seymour, J.L., Costello, C.E., Zaia, J.: The influence of sialylation on glycan negative ion dissociation and energetics. *J. Am. Soc. Mass Spectrom.* **17**(6), 844–854 (2006)
39. Karlsson, N.G., Schulz, B.L., Packer, N.H.: Structural determination of neutral *O*-linked oligosaccharide alditols by negative ion LC-electrospray-$MS^n$. *J. Am. Soc. Mass Spectrom.* **15**(5), 659–672 (2004)
40. Wada, Y., Dell, A., Haslam, S.M., Tissot, B., Canis, K., Azadi, P., Bäckström, M., Costello, C.E., Hansson, G.C., Hiki, Y., Ishihara, M., Ito, H., Kakehi, K., Karlsson, N., Hayes, C.E., Kato, K., Kawasaki, N., Khoo, K.-H., Kobayashi, K., Kolarich, D., Kondo, A., Lebrilla, C.,

Nakano, M., Narimatsu, H., Novak, J., Novotny, M.V., Ohno, E., Packer, N.H., Palaima, E., Renfrow, M.B., Tajiri, M., Thomsson, K.A., Yagi, H., Yu, S.-Y., Taniguchi, N.: Comparison of methods for profiling O-glycosylation. *Mol. Cell. Proteom.* **9**(4), 719–727 (2010)

41. Wada, Y., Azadi, P., Costello, C.E., Dell, A., Dwek, R.A., Geyer, H., Geyer, R., Kakehi, K., Karlsson, N.G., Kato, K., Kawasaki, N., Khoo, K.-H., Kim, S., Kondo, A., Lattova, E., Mechref, Y., Miyoshi, E., Nakamura, K., Narimatsu, H., Novotny, M.V., Packer, N.H., Perreault, H., Peter-Katalinić, J., Pohlentz, G., Reinhold, V.N., Rudd, P.M., Suzuki, A., Taniguchi, N.: Comparison of the methods for profiling glycoprotein glycans—HUPO human disease glycomics/proteome initiative multi-institutional study. *Glycobiology* **17**(4), 411–422 (2007)
42. Holmén Larsson, J.M., Karlsson, H., Sjövall, H., Hansson, G.C.: A complex but uniform O-glycosylation of the human MUC2 mucin from colonic biopsies analyzed by NanoLC/MS$^n$. *Glycobiology* **19**(7), 756–766 (2009)
43. Domon, B., Costello, C.E.: A systematic nomenclature of carbohydrate fragmentation in FAB-MS/MS spectra of glycoconjugates. *Glycoconj. J.* **5**, 397–409 (1988)
44. Thomsson, K.A., Karlsson, H., Hansson, G.C.: Sequencing of sulfated oligosaccharides from mucins by liquid chromatography and electrospray ionization tandem mass spectrometry. *Anal. Chem.* **72**(19), 4543–4549 (2000)
45. Shashkov, A.S., Pakulski, Z., Grzeszczyk, B., Zamojski, A.: Distribution of pyranose and furanose forms of 6-deoxyheptoses in water solution. *Carbohydr. Res.* **330**(3), 289–294 (2001)
46. Angyal, S.J.: The composition of reducing sugars in dimethyl-sulfoxide solution. *Carbohydr. Res.* **263**(1), 1–11 (1994)
47. Wertz, P.W., Garver, J.C., Anderson, L.: Anatomy of a complex mutarotation-kinetics of tautomerization of ⟼-D-galactopyranose and β-D-galactopyranose in water. *J. Am. Chem. Soc.* **103**(13), 3916–3922 (1981)